

# Seeing double: the frequency and detectability of double-peaked superluminous supernova light curves

M. Nicholl<sup>1,2\*</sup> and S. J. Smartt<sup>1</sup>

<sup>1</sup> *Astrophysics Research Centre, School of Mathematics and Physics, Queen's University Belfast, Belfast, BT7 1NN, UK*

<sup>2</sup> *Harvard-Smithsonian Center for Astrophysics, 60 Garden Street, Cambridge, Massachusetts 02138, USA*

26 October 2021

## ABSTRACT

The discovery of double-peaked light curves in some superluminous supernovae offers an important new clue to their origins. We examine the published photometry of all Type Ic SLSNe, finding 14 objects with constraining data or limits around the time of explosion. Of these, 8 (including the already identified SN 2006oz and LSQ14bdq) show plausible flux excess at the earliest epochs, which deviate by  $2\text{--}9\sigma$  from polynomial fits to the rising light curves. Simple scaling of the LSQ14bdq data show that they are all consistent with a similar double-peaked structure. PS1-10pm provides multicolour UV data indicating a temperature of  $T_{\text{bb}} = 25000 \pm 5000$  K during the early ‘bump’ phase. We find that a double-peak cannot be excluded in any of the other 6 objects, and that this behaviour may be ubiquitous. The homogeneity of the observed bumps is unexpected for interaction-powered models. Engine-powered models can explain the observations if all progenitors have extended radii or the central engine drives shock breakout emission several days after the supernova explosion.

**Key words:** supernovae: general – supernovae: individual: LSQ14bdq

## 1 INTRODUCTION

Superluminous supernovae (SLSNe) are explosions with absolute magnitudes  $M < -21$  (Quimby et al. 2011; Gal-Yam 2012). Most are hydrogen-poor, and have been termed SLSNe I or Ic. A combination of relative scarcity (Quimby et al. 2013; McCrum et al. 2015) and a preference for faint galaxies (Neill et al. 2011; Chen et al. 2013; Lunnan et al. 2014; Leloudas et al. 2015) meant that these objects went undiscovered (or unrecognised) for many years. Unbiased surveys, such as the Palomar Transient Factory (PTF; Rau et al. 2009), Catalina Real Time Transient Survey (Drake et al. 2009), Pan-STARRS (Kaiser et al. 2010), and La Silla QUEST (LSQ; Baltay et al. 2013) have fed spectroscopic follow-up to quantify their energy and origins. PTF had a built-in spectroscopic component (e.g. Vreeswijk et al. 2014), Pan-STARRS had significant 8m time for high- $z$  follow-up (e.g. Lunnan et al. 2013), and LSQ feeds the Public ESO Spectroscopic Survey of Transient Objects (PESSTO; Smartt et al. 2015), which targets SLSNe for focused study.

The light curves can be described using models powered by a central engine, such as a nascent millisecond magnetar (Kasen & Bildsten 2010; Woosley 2010), or by thermalisa-

tion of the ejecta energy in a massive circumstellar medium (Chevalier & Irwin 2011; Ginzburg & Balberg 2012). Distinguishing between these two has proved problematic despite quantitative fitting of the bolometric light curves and extensive spectra (e.g. Inserra et al. 2013).

A clue lies in the early light curve. Leloudas et al. (2012) detected a fast initial peak, or ‘bump’, in the *ugriz* light curve of SN 2006oz, preceding a 25–30 day rise to peak. Nicholl et al. (2015a) observed a similar bump, in one filter but with better time resolution, for the slowly rising LSQ14bdq. Both were interpreted as cooling emission in either CSM (Leloudas et al. 2012) or extended stellar material (Nicholl et al. 2015a; Piro 2015), with an implied radius of  $> 500 R_{\odot}$ . Kasen, Metzger & Bildsten (2015) proposed that it could be the signature of a second shock breakout, driven by a central engine in the expanding ejecta. Regardless of the mechanism, the existence of bumps in both fast and slow SLSNe is particularly interesting given that it is still unclear whether these objects form a continuum or two distinct classes (Nicholl et al. 2015b). If such bumps were ubiquitous, it would help to constrain the origin of these explosions and the progenitor structure.

This paper aims to establish whether these two bumps were special cases, or if they may in fact be common – and frequently missed by the current generation of SN surveys.

\* E-mail: matt.nicholl@cfa.harvard.edu

**Table 1.** SLSNe with early flux excesses or constraining limits

Name	$z$	Significance ( $\sigma$ ) <sup>a</sup>	$t$ -stretch <sup>b</sup>	$m$ -stretch <sup>c</sup>
LSQ14bdq	0.345	9.2, 15.8, 9.3, 10.0, 10.7	–	–
SN 2006oz	0.376	10.8, 18.3	0.43	1
PTF09cnd	0.258	4.3	0.83	1
PS1-10pm	1.206	5.5, 6.8, 3.8	0.50	0.67
PS1-10ahf	1.158	4.1	0.57	0.50
iPTF13ajg	0.740	3.6	0.63	0.48
SNLS06D4eu	1.588	9.3	0.36	0.67
SN1000+0216	3.899	5.0, 2.7	1	0.67
SN 2011ke	0.143	–	0.4	–
LSQ12dlf	0.255	–	0.7	–
SCP06F6	1.189	–	0.85	–
SNLS07D2bv	1.50	–	0.65	–
PS1-10awh	0.908	–	0.62	–
PS1-10bzj	0.650	–	0.45	–

<sup>a</sup>Deviation of the early excess (chronological); <sup>b</sup>Time stretch-factor to match LSQ14bdq light curve to data; <sup>c</sup>Magnitude stretch-factor to match LSQ14bdq.

## 2 SLSNE WITH PLAUSIBLE BUMPS

We have examined the early light curves of all published SLSNe Ic as of August 2015: see Nicholl et al. (2015b) and references therein; and of particular interest are objects in Quimby et al. (2011); McCrum et al. (2015); Howell et al. (2013); Cooke et al. (2012); Vreeswijk et al. (2014). To be useful for our study, detections or limits must exist  $> 25$  d before maximum light, in the case of fast-evolving SLSNe like SN 2006oz, or  $> 60$  d for slow-risers like LSQ14bdq.

We identify six additional SLSNe that show non-monotonic behaviour or flux excesses at the earliest epochs. Their light curves are plotted in Figure 1. Of the objects shown, only LSQ14bdq and SN 2006oz were previously recognised as double-peaked SLSNe, although Howell et al. (2013) did note a flux excess in SNLS06D4eu at early times. For the other objects, such excesses were presumably dismissed as photometric noise. However, when presented together with similar objects, it seems plausible that the earliest data points indicate a real (under-sampled) bump.

We fit the light curves (up to 30 days after maximum) with third-order polynomials and then successively remove the earliest points and re-fit, looking at the effect on  $\chi^2$  per degree of freedom (d.o.f.). When this value shows its largest decrease, we assume that we have removed the early excess from our fit. We then measure the deviation of the excluded points from this ‘bump-free’ polynomial fit, in units of  $\sigma$  (the quoted photometric error; Table 1). Additionally, we scale and overlay the light curve of LSQ14bdq (the best sampled bump detection) to test if the shape of the excess in each event is consistent with a double-peak of similar structure. The scaled light curve is not fit to the data in any formal sense – it is simply the best visual match. If data are in a similar rest-frame filter to LSQ14bdq ( $g$ -band), we allow a stretch factor in time ( $t' = t \times t_{\text{stretch}}$ ) and an additive shift in magnitude. For LSQ14bdq, the difference in  $g$ -band magnitude between the bump and main peak is  $M_{\text{bump}} - M_{\text{peak}} = 2$  mag. For higher- $z$  SLSNe with rest-frame UV photometry, the early excess (if interpreted as a

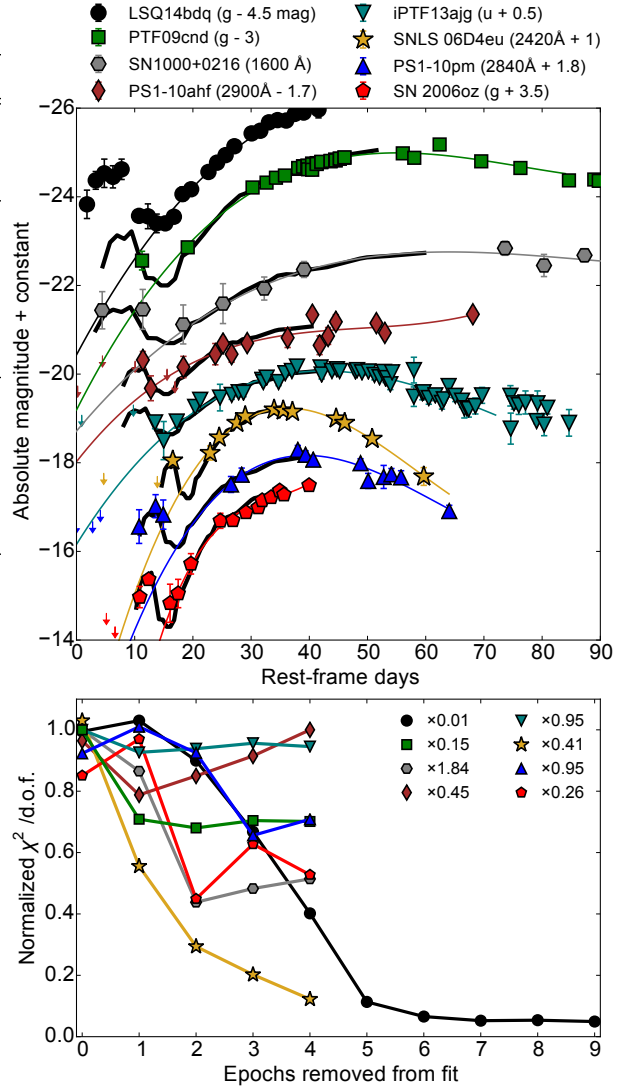


**Figure 1.** Top: Observed data and polynomial fits to the rising light curves (thin coloured lines). The thick black lines are the scaled LSQ14bdq light curves. Bottom: The reduced  $\chi^2$  for polynomial fits as early points are successively excluded from polynomial fitting. The polynomials in the top panel are those for which  $\chi^2/\text{d.o.f.}$  shows the steepest drop. Details and data sources are given in Section 2.

bump) appears to indicate  $M_{\text{bump}} - M_{\text{peak}} < 2$  mag. In such cases, we also apply a scaling factor in magnitude ( $M' = M \times M_{\text{stretch}}$ );  $M_{\text{stretch}} < 1$  flattens the light curve, reducing the brightness ratio between the two peaks.

**LSQ14bdq and SN 2006oz:** The two objects previously identified as double-peaked show marked changes in  $\chi^2/\text{d.o.f.}$ , and early excesses  $> 9\sigma$  compared to the polynomial fits, demonstrating the utility of our method. The light curve of LSQ14bdq can be mapped almost perfectly onto SN 2006oz using only a stretch in time (and simple shift in brightness). LSQ14bdq is slowly-evolving, whereas SN2006oz is a much faster SLSN (see Nicholl et al. 2015b, for discussion of the physical interpretation). The simultaneous match to both peaks with a single stretch factor suggests that the peak widths may be correlated. The excellent

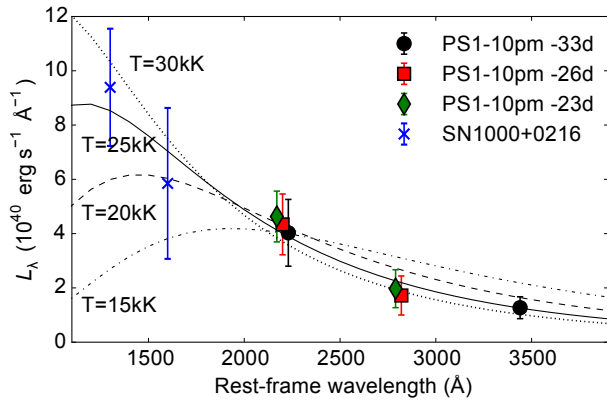


**Figure 2.** The SED of PS1-10pm compared to blackbody curves. For illustration, the blue asterisks give the FUV luminosity of SN1000+0216 during its initial peak, at around  $-50$  d.

correspondence of these two objects gives us confidence that we can assume LSQ14bdq is representative of double-peaked SLSNe, up to some stretch factor.

**PS1-10pm:** The PS1-10pm data from McCrum et al. (2015) shows flux excess in the three earliest  $r_{P1}$  points (2800 Å rest-frame for  $z = 1.206$ ) with a deviation of  $> 4\sigma$ . This was not recognised as real structure, and one could still reasonably assume a simple broad rise (albeit shallower than the subsequent decline). However, the scaled light curve of LSQ14bdq is an excellent match to the early points and rising phase. Moreover, PS1-10pm also showed significant excess in the  $g_{P1}$  and  $i_{P1}$  filters (McCrum et al. 2015). The multiple UV data points allow a blackbody SED fit and temperature estimation. Fluxes were corrected for redshift, luminosity distance and Milky Way foreground extinction. No internal galaxy extinction has been applied, since this is unknown (any host reddening would serve to increase the temperature of the fit). The SED is consistent with a blackbody of  $T_{bb} = 25000 \pm 5000$  K (Figure 2), giving the first UV measurement of the bump temperature. This is similar to the temperature of  $T_{bb} = 15000 \pm 5000$  K implied by the optical data for SN 2006oz (Leloudaz et al. 2012).

**SNLS06D4eu:** Howell et al. (2013) already noted that SNLS06D4eu showed a likely early-time excess in filters with effective wavelengths between  $\sim 2400$ -3500 Å in the rest-frame. We confirm this with both the significance of the deviation from the polynomial fit ( $9.3\sigma$ ), and a convincing match with the LSQ14bdq template, indicating that the earliest point is quite consistent with an LSQ14bdq-like bump.

**PTF09cnd:** Excluding the first point from the polynomial fit gives a clear decrease in  $\chi^2/\text{d.o.f.}$ , and indicates an excess of  $4.3\sigma$ . It can be well matched by LSQ14bdq, which it also resembles spectroscopically (Nicholl et al. 2015a; Quimby et al. 2011). We consider this a likely detection.

**PS1-10ahf:** Although the data are noisy (McCrum et al. 2015), removing the first point gives a minimum in  $\chi^2/\text{d.o.f.}$ ; the excess is then  $4.1\sigma$ . The UV light curve rise is shallow, and the optical LSQ14bdq data require a significant stretch in magnitude to match it. However, the overall shape, and detection limits, are consistent with a bump.

**iPTF13ajg:** This SLSN, from Vreeswijk et al. (2014), shows a marginal detection at best, with only a small vari-

ation in  $\chi^2$ . On the other hand, the deviation of the first point is  $3.6\sigma$  and the shape is consistent with LSQ14bdq.

**SN 1000+0216:** This object is the most distant SLSN yet detected. It was not spectroscopically classified, but we include it here because of an apparent flux excess in the rebinned  $i$ -band light curve from Cooke et al. (2012). This samples rest-frame emission at  $\approx 1600$  Å. The  $\chi^2$  test shows a sharp drop, and the resultant deviation is  $5.0\sigma$ . The shape is similar to the  $g$ -band light curve of LSQ14bdq, with no time stretch required. A magnitude stretch of 0.67 is needed, similar to factors for other UV SLSNe (Table 1). Overall, the flux differences between the first and second peaks are lower in the UV ( $\sim 1$ -1.3 mag) than in the optical ( $\sim 2$  mag). This could mean that the initial peak has a hotter effective temperature than the second. As a consistency check, we plot the rest-frame 1300-1600 Å flux of the bump of SN1000+0216 alongside the data for PS1-10pm (correcting the 1300 Å flux for Lyman- $\alpha$  absorption along the line of sight; J. Cooke, private communication). If we assume that these two SLSNe can be compared, the flux is consistent with the blackbody temperature of PS1-10pm, found to be  $T_{bb} = 25000 \pm 5000$  K in Figure 2.

### 3 SLSNE WITH NO OBSERVED BUMP

We next consider SLSNe Ic with well-observed rising phases that do not show signs of non-monotonic behaviour, but that have deep pre-detection limits to potentially exclude a bump. To act as a useful constraint, the limits must exist  $\gtrsim 25$  days before maximum light. Of equal importance is their depth; as LSQ14bdq and SN 2006oz exhibited a difference of  $\approx 2$  mag between the bump and main peak, limits must be at least this much fainter than the main peak to exclude a similar bump. Six SLSNe Ic fulfil these criteria, and are shown in Figure 3. These are SN 2011ke (Inserra et al. 2013), LSQ12dlf (Nicholl et al. 2014), SCP06F6 (Barbary et al. 2009), SNLS07D2bv (Howell et al. 2013), PS1-10awh (Chomiuk et al. 2011) and PS1-10bzj (Lunnan et al. 2013).

Following the method employed in Section 2, we fit the rise phase of each SLSN with a third-order polynomial. We then scale the light curve of LSQ14bdq to match the polynomial. However, unlike in the previous section, we do not have information on  $M_{\text{bump}} - M_{\text{peak}}$ , and therefore any scaling factor in magnitude is unconstrained. Our approach here is to use photometry in a filter as close as possible to rest-frame  $g$ -band, and scale LSQ14bdq only along the time axis, thus implicitly assuming that  $M_{\text{bump}} - M_{\text{peak}} = 2$  mag for each object. This is reasonable given the similarity between LSQ14bdq and SN 2006oz. On the other hand, since well-observed optical bumps exist for only these two objects, it is unclear what the true scatter in magnitude is.

For SN2011ke and LSQ12dlf, the observational cadence is low and the predicted bump falls at an epoch where there are insufficient data points. In the case of LSQ12dlf, the limits suggest that, if there is a bump, it may be fainter than LSQ14bdq, or have a deeper ‘dip’ between the peaks. However, earlier limits are needed to rule this out. The detection limits for the higher- $z$  SLSNe are not quite deep enough to rule out the existence of a bump. There are no other published SLSNe Ic which have enough observational data at the early times illustrated in Figures 1 and 3.

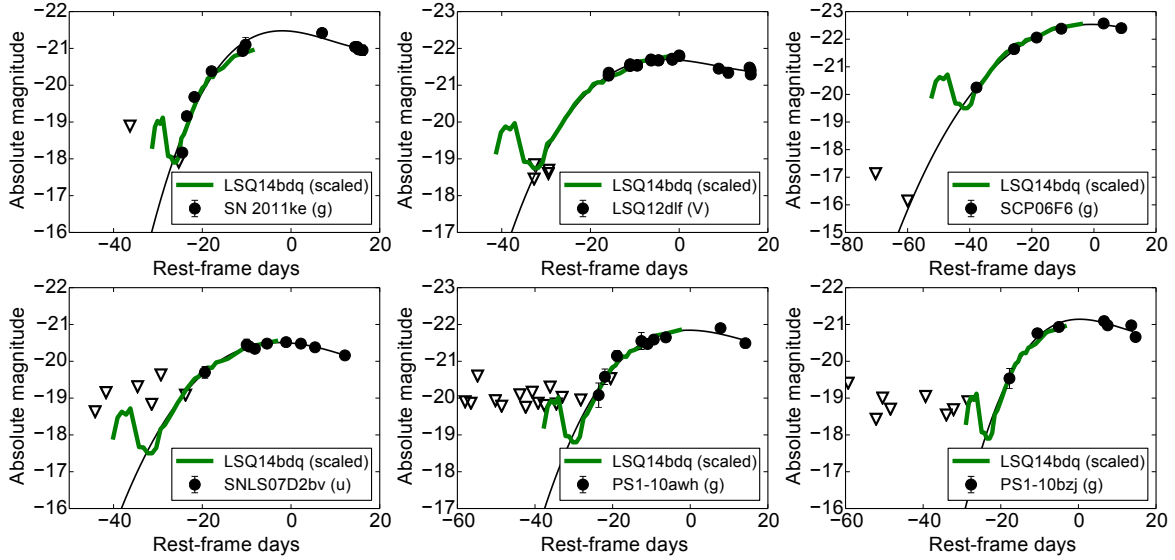


**Figure 3.** SLSNe with limiting magnitudes at  $\gtrsim 25$  d before observed maximum. The filters indicated are in rest-frame. In the top row, the cadence is insufficient to exclude a precursor peak. In the bottom row, the limits are too shallow (PS1-10bjz is marginal).

In summary, we cannot exclude the existence of a bump for *any object* to date. Where data exist that are both deep enough, and have sufficient time sampling, we see an observational signature of a bump with significance between  $2 - 9\sigma$  (compared to the observational errors). The corollary to this statement is that the current published sample of SLSNe Ic is consistent with *all* objects having a bump.

#### 4 PHYSICAL INTERPRETATION AND IMPLICATIONS

Nicholl et al. (2015b) proposed that the bump in LSQ14bdq was post-shock cooling of extended stellar material (Rabinak & Waxman 2011). Its luminosity could be recovered with reasonable explosion energy ( $E_k \sim 2 \times 10^{52}$  erg) if the progenitor had radius  $R_* \sim 500 R_\odot$  and ejected  $M_{ej} \sim 30 M_\odot$ . Piro (2015) then modelled the data using shock breakout in a different structure (employing Nakar & Piro 2014). His preferred progenitor consisted of a compact core of  $M_c \simeq 30 M_\odot$ , and a low mass envelope of  $M_e \simeq 0.3 M_\odot$  extending to  $500-5000 R_\odot$ . This model reproduced the rapid drop-off after the bump, giving a better fit to the full 10-day light curve than did the Rabinak & Waxman (2011) models. He found a similar explosion energy of  $E_k \simeq 10^{52}$  erg. The underlying physics of the two models is similar, requiring either an inflated helium/carbon-oxygen star (since no hydrogen is detected) or low-mass envelope, produced by pre-explosion activity. If bumps exist in most SLSNe, it would imply that they all have similar progenitor structure – somewhat unexpected for carbon-oxygen cores or helium stars.

In Section 2 we fitted a blackbody to the UV flux of PS1-10pm, finding  $T_{bb} = 25000 \pm 5000$  K. This is consistent with the temperature of the first peak expected by Piro (2015) of  $10000-20000$  K. Following Nicholl et al. (2015a), we fit the PS1-10pm data shown in Figure 1 with the shock cooling model of Rabinak & Waxman (2011). Assuming a blackbody SED, we apply synthetic photometry to the model in

the *HST* F250W filter, which has a similar effective wavelength to the data. A good match is obtained for very similar parameters to LSQ14bdq:  $R_* = 500 R_\odot$ ,  $M_{ej} \approx 30 M_\odot$ ,  $E_k \approx 2 \times 10^{52}$  erg. The temperature around the peak of the bump is predicted to be  $\sim 20000$  K, in good agreement with the data (Figure 2) and the predictions of Piro (2015).

The radius associated with the  $25000$  K blackbody in Figure 2 is  $\simeq 10^4 R_\odot$ . However, as the first detection is likely several days after explosion, this is not the radius of the progenitor. It could represent CSM or the extended material modelled by Piro (2015), but is also consistent with the Rabinak & Waxman (2011) fit after a few days of expansion.

Kasen, Metzger & Bildsten (2015) proposed a different model, where ejecta from a compact progenitor expand to about  $10^4 R_\odot$  after 5-10 days. If a central engine is formed (magnetar or accreting black hole) it may dynamically inflate a high-pressure bubble, propagating as a second shock. Evidence for this shock has been found in the flat velocity curves of SLSNe Ic (Chomiuk et al. 2011; Nicholl et al. 2015b). The shock breaks out from the expanding ejecta, giving an optical/UV burst lasting several days. The predicted temperature is  $T_{bb} \approx 20000$  K, the spectrum relatively featureless and blackbody-like, and there is a range of luminosities and timescales depending on the explosion/engine energies and thermalisation efficiency. This temperature (and radius) are in agreement with our measurements for PS1-10pm, and we observe a range of bump durations and luminosities (manifested in stretch factors applied to LSQ14bdq). However, in their analytic model a distinct bump is predicted only for large masses or explosion energies, or inefficient heating by the engine at early times. If bumps are common, this could be problematic for the model. Alternatively, it could place important constraints on how the magnetar energy thermalizes in the ejecta. Kasen, Metzger & Bildsten (2015) note that detailed hydrodynamical calculations are needed to investigate this further.

The time-stretch parameter used to scale the LSQ14bdq light curve preserves the relative widths of the bump and

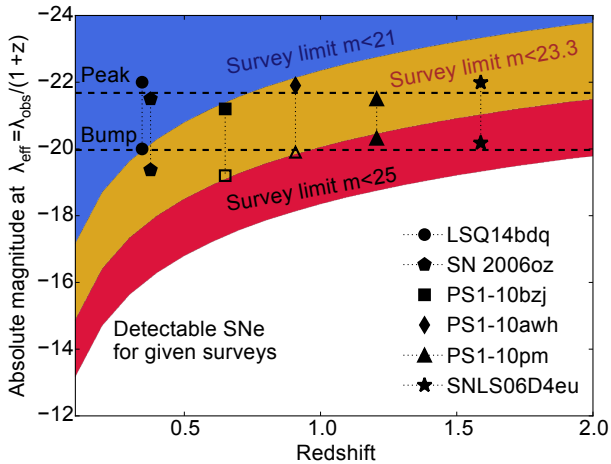


**Figure 4.** Detectability of initial and main peaks as a function of redshift. Dashed lines give mean magnitudes of observed peaks and bumps. Empty symbols are predicted bumps, assuming  $M_{\text{bump}} - M_{\text{peak}} = 2$  mag. The shaded areas show what can be observed by shallow (PTF, LSQ, PS1  $3\pi$ ), medium-deep (PS1 MDS, SDSS) and deep surveys (SNLS, DES). PS1-10bjz and PS1-10awh lie close to the PS1 MDS detectability threshold.

main peak. If this simple stretch can accommodate any SLSN light curve, it suggests that the widths of the two peaks are correlated. This could be an important discriminant between models. It is not obvious how the extended material model would produce this correlation. It may be possible to construct a model in which shock breakout occurs in circumstellar material (Ofek et al. 2010), before further interaction powers a second peak. In this case, properties of the CSM would determine the duration of both peaks, though the required structure may be rather contrived. In the Kasen & Bildsten (2010) model, the duration of the bump is linked to the diffusion and magnetar spin-down times, which also determine the time taken to rise to the main light curve peak, offering a possible explanation for the width relationship between the peaks.

## 5 CONCLUSIONS

There are 14 SLSNe Ic with published early photometry that constrains the existence of double-peaked light curves. In 8 of these, we have found at least some evidence that a bump may exist at blue and UV rest-frame wavelengths. The data for the other 6 are either too shallow or sparsely sampled to exclude bumps. We therefore propose that bumps may be ubiquitous, and that simple stretch factors map the well-sampled structure of LSQ14bdq onto all of them.

An appealing, unifying explanation is that of Kasen, Metzger & Bildsten (2015): an engine-driven shock in pre-expanded ejecta. The alternatives are the radially extended progenitor star models of Nicholl et al. (2015a) and Piro (2015), and the dense CSM interaction model of Moriya & Maeda (2012). CSM interaction models require a double-shell structure to reproduce the fast initial rise (Moriya & Maeda 2012; Nicholl et al. 2015a); it seems this would need to be remarkably homogeneous in mass, density and radius across SLSN Ic progenitors. The temperature we measure

for PS1-10pm ( $T_{\text{bb}} \simeq 25000$  K), supported by far-UV data for SN1000+0216, is consistent with both Kasen, Metzger & Bildsten (2015) and Piro (2015).

Many SLSNe have either been at too high redshift or did not have the cadence to detect the precursor peaks. Figure 4 illustrates the detectability of bumps by currently running surveys, illustrating that the Dark Energy Survey (DES) (Papadopoulos et al. 2015) has excellent potential to consistently detect bumps. For a typical  $z \sim 1$ , DES *griz* filters should anchor the rest-frame SED at  $\sim 2400$ - $4500$  Å. The next step will be to gather high-cadence early spectra.

**ACKNOWLEDGMENTS** We thank Edo Berger, Jeff Cooke, Dan Kasen, Brian Metzger, Bob Nichol and Tony Piro for helpful discussion. Funded by the European Research Council: EU(FP7/2007-2013) Grant n° [291222].

## REFERENCES

- Baltay C. et al., 2013, *PASP*, 125, 683  
 Barbary K. et al., 2009, *ApJ*, 690, 1358  
 Chen T.-W. et al., 2013, *ApJ*, 763, L28  
 Chevalier R. A., Irwin C. M., 2011, *ApJ*, 729, L6  
 Chomiuk L. et al., 2011, *ApJ*, 743, 114  
 Cooke J. et al., 2012, *Nature*, 491, 228  
 Drake A. et al., 2009, *ApJ*, 696, 870  
 Gal-Yam A., 2012, *Science*, 337, 927  
 Ginzburg S., Balberg S., 2012, *ApJ*, 757, 178  
 Howell D. et al., 2013, *ApJ*, 779, 98  
 Inserra C. et al., 2013, *ApJ*, 770, 128  
 Kaiser N. et al., 2010, in *SPIE Astronomical Telescopes+ Instrumentation*, International Society for Optics and Photonics, pp. 77330E–77330E  
 Kasen D., Bildsten L., 2010, *ApJ*, 717, 245  
 Kasen D., Metzger B., Bildsten L., 2015, *ArXiv e-prints*  
 Leloudas G. et al., 2012, *A&A*, 541, A129  
 Leloudas G. et al., 2015, *MNRAS*, 449, 917  
 Lunnan R. et al., 2014, *ApJ*, 787, 138  
 Lunnan R. et al., 2013, *ApJ*, 771, 97  
 McCrum M. et al., 2015, *MNRAS*, 448, 1206  
 Moriya T. J., Maeda K., 2012, *ApJ*, 756, L22  
 Nakar E., Piro A. L., 2014, *ApJ*, 788, 193  
 Neill J. D. et al., 2011, *ApJ*, 727, 15  
 Nicholl M. et al., 2015a, *ApJ*, 807, L18  
 Nicholl M. et al., 2014, *MNRAS*, 444, 2096  
 Nicholl M. et al., 2015b, *MNRAS*, 452, 3869  
 Ofek E. et al., 2010, *ApJ*, 724, 1396  
 Papadopoulos A. et al., 2015, *MNRAS*, 449, 1215  
 Piro A. L., 2015, *ApJ*, 808, L51  
 Quimby R. M. et al., 2011, *Nature*, 474, 487  
 Quimby R. M., Yuan F., Akerlof C., Wheeler J. C., 2013, *MNRAS*, 431, 912  
 Rabinak I., Waxman E., 2011, *ApJ*, 728, 63  
 Rau A. et al., 2009, *PASP*, 121, 1334  
 Smartt S. J. et al., 2015, *A&A*, 579, A40  
 Vreeswijk P. M. et al., 2014, *ApJ*, 797, 24  
 Woosley S., 2010, *ApJ*, 719, L204